Chemotherapy-Induced Neuropathy and Drug Discovery Platform Using Human Sensory Neurons Converted Directly from Adult Peripheral Blood

Kinga Vojnits,[a] Saleemulla Mahammad,[a] Tony J. Collins,[a] Mickie Bhatia [a,b]

Key Words. Direct conversion sensory neurons • High-content screening platform • Chemotherapy-induced neurite degeneration

[a]Stem Cell and Cancer Research Institute, Michael G. DeGroote School of Medicine, McMaster University, Hamilton, Ontario, Canada; [b]Department of Biochemistry and Biomedical Sciences, McMaster University, Hamilton, Ontario, Canada

Correspondence: Tony J. Collins, Ph.D., Stem Cell and Cancer Research Institute, McMaster University, Michael G. DeGroote Centre for Learning, 1280 Main Street West, MDCL 5107, Hamilton, Ontario L8S 4K1, Canada. Telephone: (905) 525-9140 x 21791; e-mail: tjc@mcmaster.ca; or Mickie Bhatia, Ph.D., Stem Cell and Cancer Research Institute, McMaster University, Michael G. DeGroote Centre for Learning, 1280 Main Street West, MDCL 5029, Hamilton, Ontario L8S 4K1, Canada. Telephone: (905) 525-9140 x 28687; e-mail: mbhatia@mcmaster.ca

Abstract

Chemotherapy-induced peripheral neuropathy (PN) is a disorder damaging the peripheral nervous system (PNS) and represents one of the most common side effects of chemotherapy, negatively impacting the quality of life of patients to the extent of withdrawing life-saving chemotherapy dose or duration. Unfortunately, the pathophysiological effects of PN are poorly understood, in part due to the lack of availability of large numbers of human sensory neurons (SNs) for study. Previous reports have demonstrated that human SNs can be directly converted from primitive CD34^{+} hematopoietic cells, but was limited to a small-scale product of SNs and derived exclusively from less abundant allogenic sources of cord or drug mobilized peripheral blood (PB). To address this short-coming, we have developed and report detailed procedures toward the generation of human SN directly converted from conventionally drawn PB of adults that can be used in a high-content screening platform for discovery-based studies of chemotherapy agents on neuronal biology. In the absence of mobilization drugs, cryogenically preserved adult human PB could be induced to (i)SN via development through expandable neural precursor differentiation. iSNs could be transferable to high-throughput procedures suitable for high-content screening applicable to neuropathy for example, alterations in neurite morphology in response to chemotherapeutics. Our study provides the first reported platform using adult PB-derived iSNs to study peripheral nervous system-related neuropathies as well as target and drug screening potential for the ability to prevent, block, or repair chemotherapy-induced PN damage. STEM CELLS TRANSLATIONAL MEDICINE 2019;8:1180–1191

Significance Statement

This study uses converted human sensory neurons generated from adult peripheral neuropathy samples. This chemotherapy-induced peripheral neuropathy possesses key advantages to human sensory neurons derived from pluripotent stem cells based on comparative side-by-side analysis and could be transferable to robust high-throughput procedures suitable for drug screening.

Introduction

Peripheral neuropathy (PN), a disorder damaging the peripheral nervous system (PNS), negatively impacts the quality of life by causing weakness, numbness, pain, or altered sensation in patients, and remains one of the most prevalent neurologic conditions encountered by physicians [1, 2]. PN is a widespread disorder estimated at 2.4% of the world population with prevalence increasing to 8% with aging [1, 3]. Over 100 types of PN have been defined and diagnosed [4], each with its own symptoms and prognosis; however, in many cases, a specific cause cannot be identified. A large subset of PNs, however, are caused by chemotherapeutic agents [5], as a progressive and dose-dependent side effect of cancer treatment, affecting 30%–40% of chemotherapy-treated patients [6]. The chemotherapy effects and PN outcomes vary between different classes of drugs; the most neurotoxic classes of anticancer drugs are taxanes and platinum-based compounds [7]. In severe cases, pain experienced, sensory changes, and weakness can lead to dose reductions in chemotherapy protocols, which negatively impacts the chemotherapy treatment outcomes that prevent remission induction [8–11]. Currently, there is no treatment cure for PN, and the existing medications are limited to generic antipain medications, including general antidepressants, anticonvulsants, opioid therapies, and nonsteroidal anti-inflammatory drugs [5, 12], which simply numb the nervous system and are not PNS-specific in target or drug behavior [13, 14].

A major obstacle in developing new-in-class direct therapies is the poor foundational

understanding of the pathophysiology of chemotherapy-induced PN in a tractable manner, which allows for the identification of new targets, probes, and candidate drugs [6]. To date, the cellular pathophysiology of the disease has predominantly been investigated using rodent cellular models. However, reported limitations of these models [15–18] and biological differences between rodent and human physiology [19] limit translatability between the species and the fundamental pathways of chemotherapy-induced PN remain unknown. Thus, large-scale generation of human sensory neurons (SNs) is an imperative to engineer therapeutics that target and attenuate chemotherapy-induced PN condition. The lack of accessibility of human specific neural tissue (both living and post-mortem) and the inability to generate sufficient human peripheral neuronal models in vitro has been the bottleneck in developing reliable assays for this kind of drug screening.

Although recent advances in cellular reprogramming to pluripotent state or by direct conversion of accessible patient specific cell types to SN [20] have provided new alternative tools for generating human cell types that are difficult to procure [21–23], there is no validated and scalable platform available for efficient generation of functional peripheral neurons. For example, the creation of neural cells differentiated from human pluripotent stem cells (embryonic stem cells or induced pluripotent stem cells; PSCs) is time-consuming, laboratory-intensive, and difficult to scale up. Moreover, the problems with PSCs' line-to-line differentiation variability, karyotype instability, and the remaining undifferentiated tumor-forming pluripotent cells within the differentiated cells of alterative cells types and lineages in cultures have yet to be fully resolved [24–26]. Other methods to derive neurons by single conversion step without PSC formation from adult tissues, such as fibroblasts [22, 27–32], urinary cells [33], or cord blood [34, 35], are accompanied by other limitations, for example, human skin biopsies that are difficult to obtain and are not available from historical clinical studies, or the requirement of multiple transcription factors, and only inefficiently give rise to functional neurons, and rarely to those of the PNS [34, 36]. Here, we detail platform development of a high-content screening system for assaying chemotherapy-induced PN using patient specific human iSNs directly converted from nonmobilized adult peripheral blood (PB) for the study of PNS-related neuropathies.

MATERIALS AND METHODS

Cell Culture and Derivation of Human Induced Neural Progenitor Cells

To derive induced neural progenitor cells (iNPCs), our previously published protocol was followed [34]. Briefly, two PB donor samples of approximately 325 M viable mononuclear cells (MNCs) were obtained from Stemcell Technologies (Vancouver BC, Canada) (catalog no. 70025, lots: #1510080039 and #1509220012). The MNC populations were labeled with anti-CD34-conjugated magnetic microbeads according to the manufacturer's instructions (Miltenyi Biotec, Bergisch Gladbach, Germany). The cell suspension was then loaded onto a MACS LS Column (Miltenyi Biotec) that is placed in the magnetic field of a MACS Separator. Separated CD34$^+$ MNCs were expanded and cultured in Iscove's Modified Dulbecco's medium (IMDM; Invitrogen, Waltham MA, USA) containing 15% fetal bovine serum

(HyClone, Mississauga ON, Canada), 1× bovine serum albumin/recombinant human insulin and human transferrin, 1× sodium pyruvate, 0.5% L-glutamine, 25 ng/ml interleukin 3 (IL3), 100 ng/ml human stem cell factor, 100 ng/ml FMS-like tyrosine kinase 3 ligand, and 100 ng/ml thyroid peroxidase for 3 days. All reagents were purchased from R&D System (Oakville ON, Canada) unless otherwise stated (Supporting Information Experimental Procedures).

Lenti-virus OCT4 delivery system was used for generation of iNPCs from the cultured CD34$^+$ MNCs from each donor. CD34$^+$ MNCs were cultured in CD34$^+$ expansion medium along with 10 μM SB431542 (Stemgent, Beltsville MD, USA), 100 nM LDN-193189 (Stemcell Technologies) and 3 μM CHIR99021 (Stemcell Technologies), and lenti-virus OCT4. The medium containing virus was replaced with fresh CD34$^+$ expansion medium 24 hours after infection. Forty-eight hours after infection, cells were transferred to irradiated MEFs and the culture medium replaced with Dulbecco's modified Eagle's medium (DMEM)/F12 medium (Invitrogen) containing 20 ng/ml basic fibroblast growth factor (bFGF; Corning) and 20% knockout serum replacement (ThermoFisher Scientific, Waltham MA, USA). After 3 days, culture medium was replaced with neural precursor medium (NPC medium) that contained basal medium (DMEM/F12 [Invitrogen], 1× N2 [ThermoFisher Scientific], 1× B27 [ThermoFisher Scientific]) supplemented with 10 μM SB431542 (Stemgent), 100 nM LDN-193189 (Stemcell Technologies), 3 μM CHIR99021 (Stemcell Technologies). After 10–14 days, neural precursors-like colonies were manually picked, transferred to poly-ornithine/laminin-coated culture plates for propagation with NPC medium supplemented with 20 ng/ml bFGF (Corning, New York, USA), and 20 ng/ml epidermal growth factor (EGF) (R&D System). Primary neurosphere culture was used to further enrich iNPCs (Supporting Information Experimental Procedures).

Human iNPC Differentiation

For nociceptive sensory neuron differentiation [34, 37–39], iNPCs were cultured in sensory neuron specification medium (snSpec medium) contained of basal medium supplemented with 10 μM N-[N-(3,5-Difluorophenacetyl)-L-alanyl]-S-phenylglycine t-butyl ester (DAPT) (Sigma–Aldrich, Oakville ON, Canada), 1 μM SU5402 (Stemcell Technologies), and 3 μM CHIR99021 (Sigma–Aldrich). After 7 days, media was changed to sensory neuron maturation medium (snMat medium) contained of basal medium supplemented with 10 ng/ml brain derived neurotrophic factor (BDNF) (ThermoFisher Scientific), 10 ng/ml glial cell-derived neurotrophic factor (GDNF) (ThermoFisher Scientific), 10 ng/ml nerve growth factor (NGF) (Stemcell Technologies), 10 ng/ml neurotrophin-3 (Stemcell Technologies), 200 μM ascorbic acid (Sigma–Aldrich), and 5 μM forskolin (Abcam, Toronto ON, Canada) for 7–14 days until the desired maturation stage for a given experiment (Supporting Information Experimental Procedures).

Immunofluorescence

Cells were fixed and washed using the BD Cytofix/Cytoperm Fixation/Permeabilization solution kit (ThermoFisher Scientific) containing 4% paraformaldehyde. Cells were incubated with appropriate primary and fluorochrome-conjugated secondary antibodies, and then counterstained with Hoechst 33342 (Invitrogen). The following antibodies were used: PAX6 (BD Biosciences, San Jose CA, USA), NeuN (Abcam, Toronto ON, Canada), Nestin, TUJ1, SOX2, MAP2 (R&D System), BRN3a, P2X3R, Peripherin (PRPH;

EMD Millipore, Etobicoke ON, Canada), GABA, and GFAP (Sigma–Aldrich).

Flow Cytometry

Cells were fixed using the BD Cytofic/Cytoperm Fixation/Permeabilization solution kit (ThermoFisher Scientific), including 4% paraformaldehyde. Fixed cells were stained with CD34, CD45, Nestin, SOX2 (R&D System), and PAX6 (BD Biosciences). Unconjugated antibodies were visualized with appropriate fluorochrome conjugated secondary antibodies. Fluorescence-activated cell sorting (FACS) analysis was performed on a FACSCalibur cytometer (Becton Dickinson Immunocytometry Systems) and analyzed using the FlowJo software (Tree Star Inc., Ashland OR, USA).

Calcium Imaging

Differentiated mature iSNs were loaded with Fluo-4-AM fluorescence dye (Invitrogen) by incubating at room temperature for 1 hour followed by 45 minutes period for de-esterification. Cells were washed and incubated in Hanks' balanced salt solution, supplemented with 25 mM HEPES buffer and 5.5 mM glucose. Calcium flux was monitored using an Olympus IX81 inverted epifluorescence microscope (Olympus, Markham, ON, Canada) coupled to a xenon arc lamp (EXFO, Quebec, QC, Canada). Indicated agonists, α,β-meATP and capsaicin, were diluted in the aforementioned solution for a final stimulation concentration of 30 μM for α,β-meATP and 1 μM for capsaicin. Fluorescence images were collected using an EMCCD (Electron Multiplying Charged Coupled Device) camera (Photometrics, Tucson, AR, USA) every 2 seconds through a GFP filter cube (Semrock, Rochester, NY, USA). Off-line analysis of the intensity pattern of Fluo-4 signal was performed in ImageJ (NIH, Bethesda, MD, USA).

Preparation of Compounds

All compounds as libraries were purchased from suppliers, Taxol (Prestwick Chemical Library), Etoposide, Vincristine sulfate, Cisplatin, and Bortezomib (Ontario Institute for Cancer Research Collection), as 10 mM stocks in Dimethyl Sulfoxide (DMSO). At 10 mM, we did not observe insolubility and precipitation with any compounds upon visual inspection. Compounds were stored at -80°C. Test compounds were prepared in a 10-fold dilution scheme, 10 μM as the highest concentration. The concentration range for all compounds was 0.01–10 μM (final concentration of DMSO in the culture medium was 0.1%). Compounds were screened in quadruplicate at each concentration on the same plate.

Cell Viability Assay

Resazurin reduction assay was used to determine cell viability in three biological replicates. After 48 hours of drug exposure, medium was removed and replaced with 100 μl of freshly prepared 10 μg/ml solution of resazurin (Sigma–Aldrich) in snMat medium. The cells were incubated for 2 hours at 37°C and 5% CO_2. Fluorescence signal at 544 nm excitation/590 nm emission was measured using a microplate reader.

High-Content Imaging and Neurite Length Analysis

After 48 hours of drug treatment, cells were stained with Calcein green and Hoechst 33342 at room temperature for 20 minutes for live cell imaging. Images were acquired at 20× with an automated high-content confocal fluorescence microscopy (Operetta, PerkinElmer, Woodbridge ON, Canada) by means of epifluorescence illumination and standard filter sets, and 15 fields were evaluated for each well. Drug treated cultures were compared with time-matched, untreated controls. Image analysis was performed by using custom scripts in the Acapella software (PerkinElmer). Hoechst was used to identify and count individual nuclei in channel 1 and calcein green was used in channel 2 to identify cell bodies and neurites by intensity. Images and well-level data were stored and analyzed in a Columbus Database (PerkinElmer).

Statistical Analysis

A minimum of three biological replicates was established for each of the described experiments. Statistical analyses were carried out using GraphPad Prism version 7.0a (Graph Pad Software, Inc., San Diego CA, USA). All numerical data were expressed as mean values ± SEM or ±SD. Comparisons between two groups were performed by using unpaired two-way or one-way Students' t test assuming two-tailed distribution, and unequal variances. For multiple comparisons, ANOVA or Kruskal-Wallis test was applied. Statistical significance was considered at $p < .05$, where *, $p = .05$ and **, $p = .01$.

RESULTS

Direct Conversion of Human PB to Neural Precursors

In the absence of iPSC formation, reprogramming of human blood to alternate nonhematopoietic cell fates has been widely reported [34, 35, 40–42], where reprogramming arises exclusively from rare CD34^{+} hematopoietic stem/progenitor subsets. In all cases, however, the source of human blood has been either cord blood or adult sources using PB stem/progenitor cells after drug administration of mobilizing agents [40–42]. A more practical source of blood would be nonmobilized PB that can be readily obtained from patients and/or abundantly available from cryopreserved hematopoietic cells in tissue banks from clinical trials or other studies. However, the low frequency of CD34^{+} stem/progenitor cells in healthy adult PB introduces a major obstacle is using this source of somatic cells for cell fate conversion. To establish a robust and reproducible protocol for acquiring neural cells through highly proliferative iNPCs, we developed an approach to reprogram adult PB, containing only low frequency of CD34^{+} cells, which can be readily obtained from adults. To establish a practical and predictable platform for optimization, we quantified frequencies and cell yields along the multiple steps from adult PB to iSNs reprogramming.

MNC from adult PB were labeled with anti-CD34-conjugated magnetic MicroBeads, and then loaded onto a MACS LS Column for separation and elution enrichment of CD34^{+} cells (Fig. 1A). Adult PB donor samples of approximately 325 M viable MNCs yielded 0.1% CD34^{+} cells (0.09% from donor 1 and 0.11% from donor 2; Fig. 1B, Supporting Information Fig. S1A). Quantification of PB before and after separation revealed a 50% recovery of input CD34^{+} from the column and a 10-fold enrichment of CD34^{+} in the output cells. Culture of these cells in IMDM medium for 3 days resulted in an average 2.5-fold expansion from the original MNC population (88% and 90% CD34^{+} cells from donor 1 and 2, respectively, Fig. 1B, Supporting Information Fig. S1A). Overall, this equated to the yield of approximately 1 M CD34^{+} cells after initiation separation and 3 days of culture.
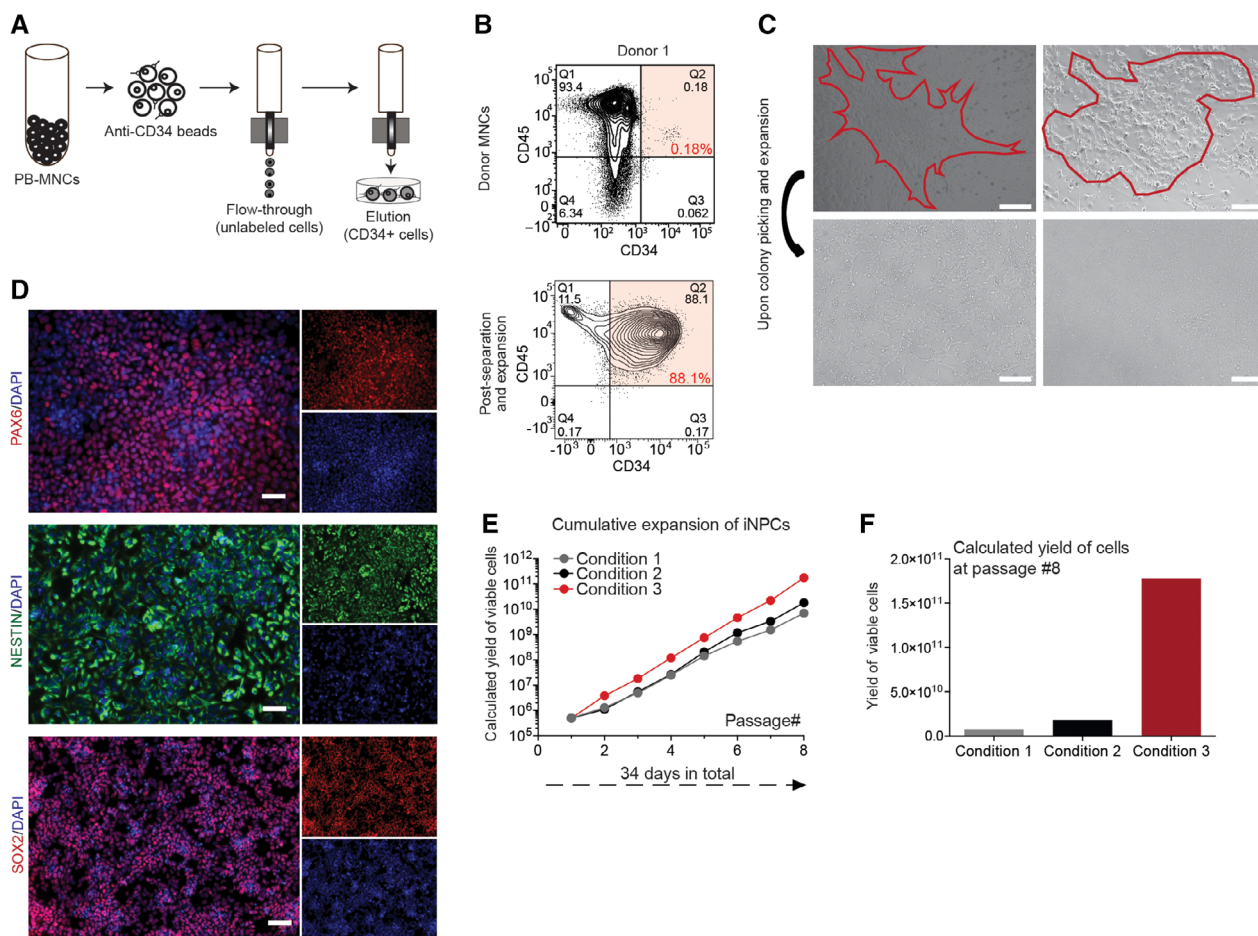
Figure 1. OCT4 mediated direct conversion of human peripheral blood samples to neural precursor cells. **(A):** Schematic for separation and elution of CD34+ mononuclear cells (MNCs). **(B):** Flow cytometry plots of MNCs from donor 1 prior (top row) to and after isolation and expansion of CD34+ population (bottom row). **(C):** Phase contrast images of two example iNPC colonies 10 days after OCT4 transduction (top row) and after colony picking and expansion (bottom row). Scale bar represents 300 μM. **(D):** Validation of induced neural progenitor cells (iNPCs) after 12 weeks of initial OCT4 infections of CD34+ cells. Derived iNPCs were plated in 24-well plates (100K seeding) and were fixed and stained for PAX6, Nestin, and SOX2 in combination with staining for DNA (Hoechst). Scale bar represents 50 μM. **(E):** Evaluation of iNPC expansion over multiple passages and in multiple culture conditions. The potential yield of iNPCs over multiple passages and in multiple conditions (medium and substrate) was calculated. **(F):** After eight passages, iNPCs yielded 25× greater cell number in culture conditions developed in house, in condition 3.

With our established and previously reported OCT4 lentiviral delivery procedure, combined with SMAD + GSK-3 inhibition [34], iNPC-like clusters appeared within 2 weeks in NPC cell medium [43] from the transfected CD34+ PB cultures. These clusters were recognizable as tightly packed neurosphere-like small colonies (Fig. 1C). Although the efficiency of viral transduction was low and differed between the donors (1:25,000, 1:9,000 efficiency in donor 1 and 2), the resulted 3%–9% OCT4+ cells gave rise to 2–4 NPC colonies per initial 100K PB MNCs. Colonies were isolated manually and further expanded on polyornithine/laminin coated 24-well plates in NPC medium (Fig. 1C). Human iNPCs were identified by detected expression of PAX6, Nestin, and SOX2 in situ staining (Fig. 1D). There was no difference in PAX6, SOX2, and Nestin staining of iNPCs from the different adult PB donors. Human iNPCs were passaged as single cells by accutase enzyme treatment when they reached confluence (approximately 4 days of culture) yielding 500K cells per well and reseeded at 100K per well. To further scale-up the cultures and to identify the optimal expansion conditions, we evaluated the iNPC cultures over multiple passages and three specific conditions

(Table 1, Fig. 1E) [44]. Culture conditions developed by our lab reported here (Table 1, condition 3) were found to be optimal for expansion, yielding 25× greater number of iNPCs after eight passages (Fig. 1F) than the other two methods and formats for NPC expansion we tested (Table 1, condition 1 and 2) [45–48]. In all conditions, cells retained their PAX6, Nestin, and SOX2 expression indicating that the cultures are broadly stable and not prone to differentiation (Supporting Information Fig. S1B). Over a period of 8–10 weeks in iNPC expansion, culture represented a yield of 300–400 M cells from a single original iNPC derived colony.

Sensory Neuron Differentiation of Directly Converted Neural Precursors

Using combined small-molecule inhibition (SU5402, DAPT, and CHIR99021) to induce sensory neuron (nociceptors; iSNs) differentiation [34] of the directly converted human iNPCs, confluent (90%) iNPCs were further cultured in sensory neuron specification medium (snSpec medium) for 7 days, and then switched to sensory neuron maturation medium (snMat medium) for

Table 1. Different culture conditions tested for iNPCs expansion

Condition 1	Condition 2	Condition 3
RHB-A basal medium	DMEM/F12 basal medium	DMEM/F12 basal medium
N2 (1×)	N2 (1×)	N2 (1×)
B27 (1×)	B27 (1×)	B27 (1×)
bFGF (10 ng/ml)	bFGF (20 ng/ml)	bFGF (20 ng/ml)
EGF (10 ng/ml)	EGF (10 ng/ml)	EGF (10 ng/ml)
Poly-L-ornithine-laminin coated plates	Poly-L-ornithine-laminin coated plates	Matrigel coated plates

7–14 days to achieve mature and functional iSNs (illustrated in Fig. 2A). To evaluate the phenotype of these iSNs, we assessed the expression of protein markers specific for nociceptors. Nearly all iSNs expressed generic neuronal markers, MAP2 and the pan-neuronal marker Tuj1, and had a neuronal-like morphology with long branching axons (Fig. 2B). At the protein level, human iSNs expressed nociceptor specific markers PRPH, purinergic receptor (P2RX3), and BRN3a, a class IV POU domain-containing transcription factor highly expressed in the developing peripheral sensory nervous system, and the intermediate filament NF200, a marker of myelinated nociceptors (Fig. 2B). No qualitative or phenotypic difference between the iSNs derived from different donors/clones was observed. It is known that neural cell type mosaicism dramatically affects the reproducibility of neuronal response. As such, we extended phenotype profiling of resulting iSN cultures to determine the degree of mosaicism in the culture by staining for central nervous system (CNS) specific and glial markers, GABA and GFAP (Fig. 2C). Human iSN cultures were positive for the neuronal marker MAP2 but negative for cells expressing GABA$_B$-R1 that is associated with CNS neurons and the glial marker GFAP (Fig. 2C). Moreover, quantification of NeuN+ (97.4%), Tuj1+ (99.9%), and PRPH+ (94.1%) cells demonstrated that the cultures are highly enriched for neuronal cells (Supporting Information Fig. S2A), in our iSN cultures directly converted from adult PB. In contrast, hPSC-derived CNS cells were heterogeneous cultures with a lower frequency of Tuj+ cells (76.82%; Supporting Information Fig. S2A). These results reveal reprogrammed adult PB samples can give rise to large-scale highly purified cultures of human nociceptive neurons.

To confirm the successful sensory neuronal differentiation of iNPCs to resulting iSNs, we evaluated response to α,β-methylene-ATP (α,β-meATP), a selective agonist of P2RX3, using calcium flux. As the α,β-meATP-sensitive P2RX3 receptors play an important role in triggering nociceptive signals, a functional assay measuring α,β-meATP-induced intracellular calcium concentration transients has been widely used to evaluate the response of nociceptors to painful stimuli [49, 50]. Consistent with previous results with cord-blood converted iSNs, iSNs converted from adult nonmobilized PB exhibited robust elevation of cytosolic calcium in to α,β-meATP treatment (Fig. 2D). Thus, our differentiation protocol yielded bona fide nociceptors from directly converted neural precursors obtain from adult PB.

Crucial to establishment of this technology as a high-throughput platform is the ability to cryopreserve cells for storage and scalability. To ensure the highest viability, proper reattachment and maintenance of differentiation capacity of iNPCs post-thaw, we have extensively characterized the optimal cryopreservation protocol using cells at this stage of direct reprogramming. We have identified accutase treatment as critical in the cryopreservation protocol, the optimal treatment duration should be between 5 and 10 minutes (as detailed in procedural Materials and Methods section). Several alternate cryopreservation medium were evaluated, for example, medium 1 (DMEM/F12 + 10% DMSO), medium 2 (DMEM/F12 + N2 + B27 + 10% DMSO), medium 3 (snMat medium +10% DMSO), all with less than 50% recovery but no affects to recovered iSN morphology (Fig. 2E, Supporting Information Fig. S2B). These results indicate that the optimized cryopreservation protocol yielded approximately 80% viable cells post-thaw was found to yield only half that for mature iSNs (Fig. 2F).

Comparative Characterization of iSNs for High-Content Screening

We next aimed to optimize conditions for 96-well plate seeding to generate functional iSNs derived from adult PB. It has been reported before that the inhibition of the Rho/Rho-kinase (ROCK) pathways enhanced neurite outgrowth in spinal cord injury models in vivo [51–53] and in neural stem cells differentiation in vitro [54]; and reduced apoptosis of neural precursors in culture [55] as well as during transplantation [56]. Human iSNs were specified (7 days) and matured (24 days) in 24-well plates prior to reseeding to 96-well plate with or without Y-27632 (ROCK inhibitor, ROCKi). Seeding densities of 10K, 25K, and 50K cells per well were comparatively evaluated in the absence of ROCKi (Control, CNT) or with ROCKi present for the initial 24 hours after seeding (24 hours ROCKi) versus the presence of ROCKi for the entire duration of culture (7 days ROCKi). Culture media was changed 24 hours after seeding, then again at day 3 and day 6. After 7 days of culture, cells were stained with Hoechst and the vital-dye Calcein-AM (Fig. 3A) and quantified using high-content imaging. Image analysis showed that there was a linear relationship between seeding density and viable cells at 7 days after seeding (Fig. 3B). Presence of ROCKi significantly increased the number of viable cells by 30% at seeding density of 50K per well. Further experiments showed that seeding densities of 100K cells per well or higher (Supporting Information Fig. S3A, S3B) resulted in no cell survival; that was independent of the presence of ROCKi. Quantification of cell morphology revealed that treatment with ROCKi increased average neurite length per cell for seeding densities of 10K and 25K per well; whereas inclusion of ROCKi for the 7 days of culture the average neurite length increase compared with untreated controls for all of the seeding densities tested (Fig. 3C). Differentiated iSNs in 96-well plates showed typical morphology and phenotype for nociceptors and they highly expressed PRPH and P2RX3 (Fig. 3D). These results indicate ROCKi promotes cell survival during seeding of iSNs into 96-well formats directly converted from adult PB.
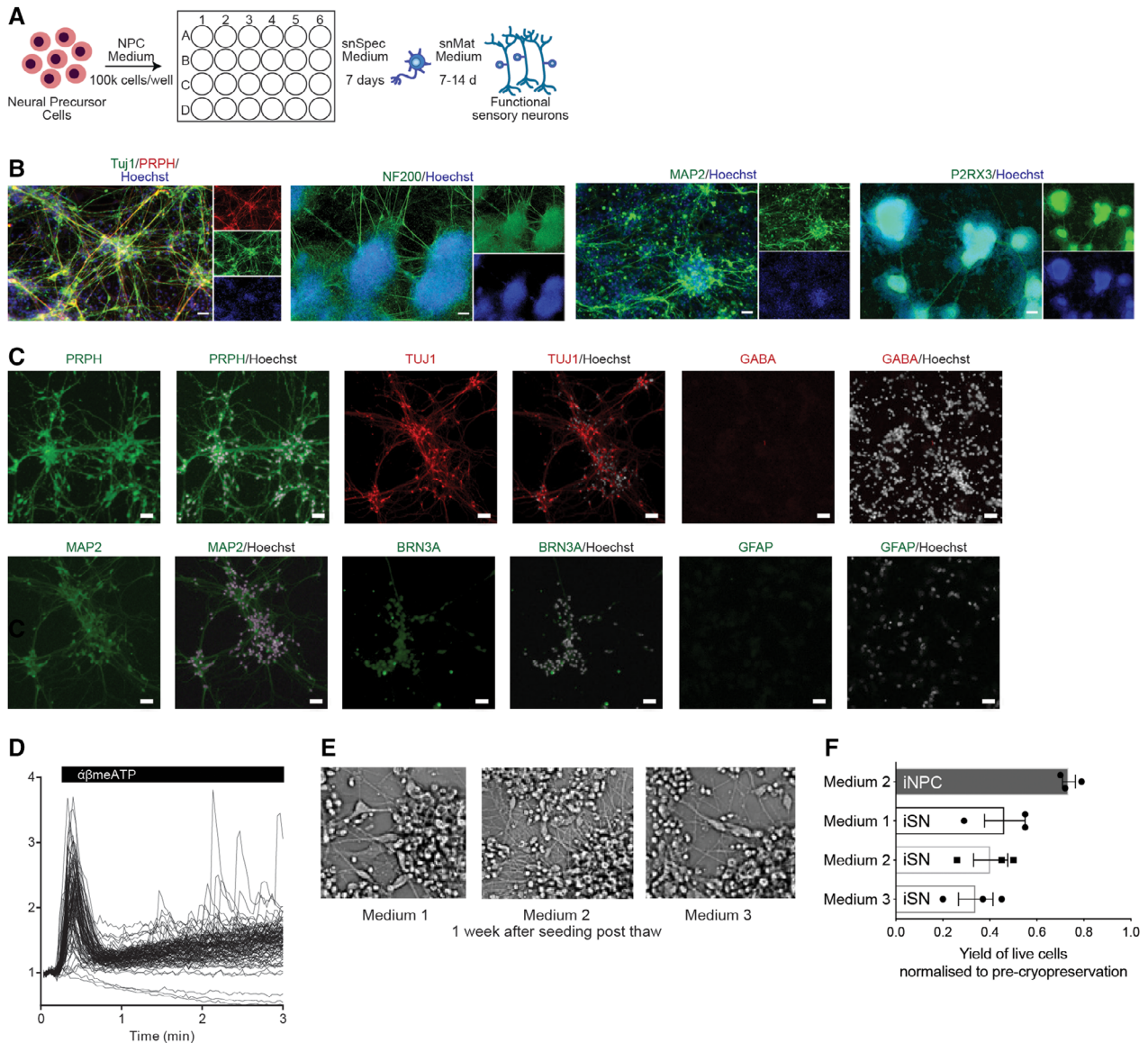
Figure 2. Sensory neuron differentiation of direct conversion neural precursor cells. **(A):** Schematic of sensory neural differentiation protocol from peripheral blood-derived induced neural progenitor cells (iNPCs). **(B):** Immunofluorescence images of 21 day differentiated induced sensory neurons (iSNs). Cells were fixed and stained for peripheral nervous system (PNS) markers, Tuj1, PRPH, NF200, MAP2, and P2RX3. Nuclei were stained with Hoechst. Scale bar represents 50 μM. **(C):** Immunostaining of iSNs cultures with PNS specific, CNS specific and glial markers, PRPH, Tuj1, MAP2, GABA, BRN3a, and GFAP. Scale bar represents 50 μM. **(D):** Calcium trace and distribution of cells in response to 30 μM α,β-meATP treatment. **(E):** Phase contrast images of iSNs 1 week post-thaw for different cryopreservation medium. **(F):** Optimization of cryopreservation of iNPCs and iSNs. Yield of viable cells after cryopreservation in various medium. Mean ± SD for three independent experiments.

To characterize maturation function of iSNs in 96-well format, we analyzed cytoplasmic calcium levels during treatment with agonist response, capsaicin (1 μM), or α,β-meATP (30 μM). Agonist response was quantified as follows: cells were AM-ester loaded with the calcium-sensitive dye Fluo4-AM and imaged during treatment with either the SN-agonists α,β-meATP or capsaicin. The peak fluorescence response (normalized to resting levels) F/F0 of individual cells was plotted (Fig. 3E). Cells showing a peak signal >1.75 basal was classified as having responded to agonist treatment. Quantification of the frequency of cells responding to each agonist showed some general trends from these data. Three extra days duration did not dramatically affect cells when seeded at 50K, although it did increase the frequency of cells responding to agonist when cells were seeded

at 25K. ROCKi treatment for 24 hours resulted in increased agonist response at 7 days and inclusion of ROCKi for the entire culture duration improved this response.

Comparison of Directly Converted iSNs to iPSC-Derived iSNs in High-Content Formats

One of the main advantages of direct conversion from PB to iSN is the rapid and practical achievement of sufficient quantities of purified iSNs in the absence of alterative lineages and cell types, as well as residual undifferentiated stem cells that arise using hPSCs. Beyond these parameters, we sought to comparatively determine the overall quality of directly converted iSNs functionally versus SNs derived from human iPSCs. Mature peripheral-like neurons, Peri.4U neurons from Axiogenesis
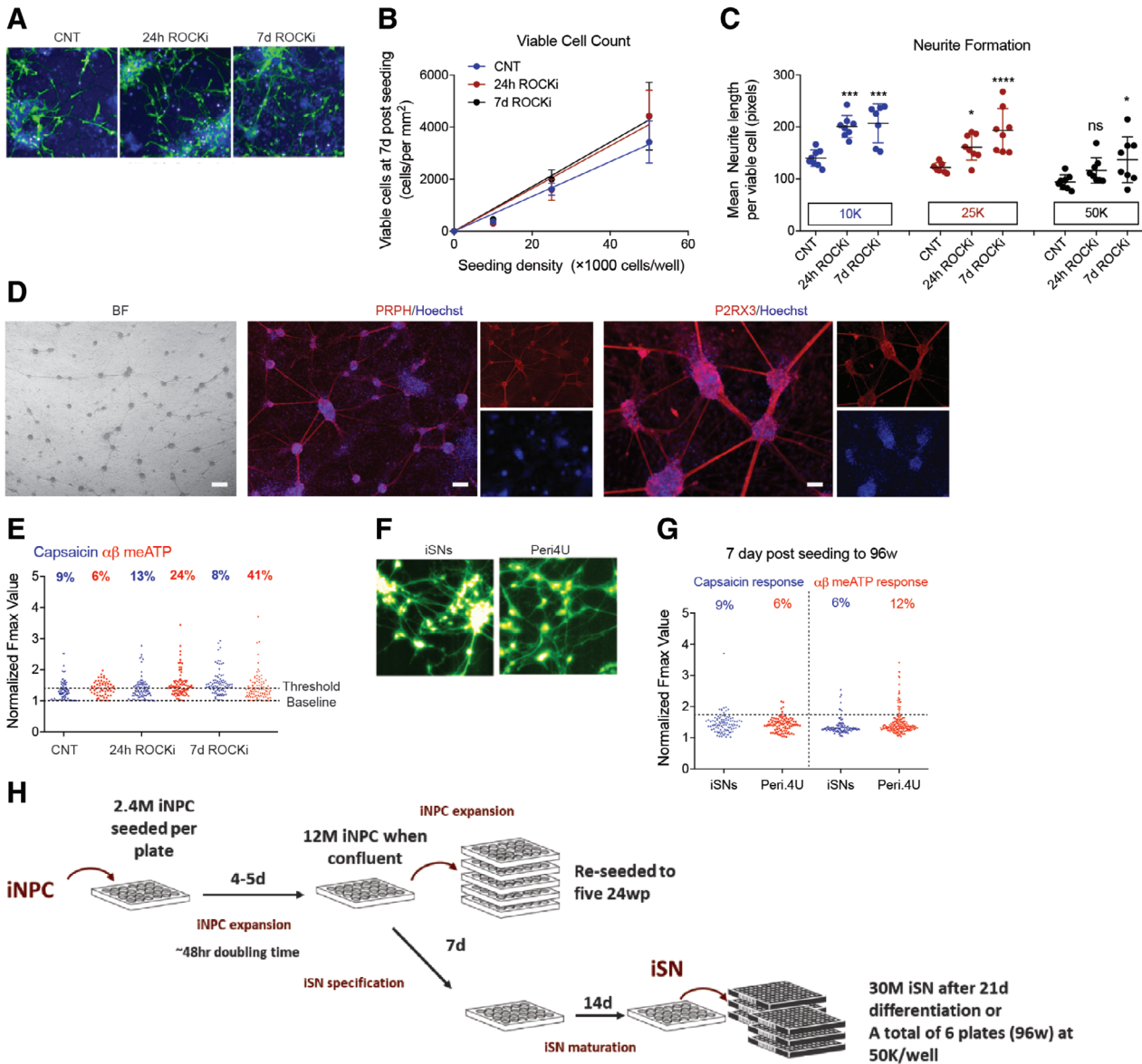
Figure 3. High throughput of induced sensory neurons for screening purposes. **(A):** Calcein green and Hoechst staining of induced sensory neurons (iSNs) with ROCKi absent (Control, CNT) or present for 24 hours (24 hours ROCKi) or the entire culture period (7 days ROCKi). **(B, C):** Quantified viable cell yield and neurite formation at 7 days post-seeding by high-content analyses. Statistical significance was considered at p < .05, where *, p = .05; ***, p and ****, p < .001. **(D):** Phase contrast and immunostaining images of 7 days matured iSNs in 96-well plates. Cultures were stained highly positive for peripheral nervous system specific markers, Peripherin (PRPH, red), and purinergic receptor (P2RX3, red, right panel). Nuclei were stained with Hoechst (blue). Scale bar represents 50 μM. **(E):** Peak calcium flux in response to 1 μM capsaicin and 30 μM α,β-meATP treatment of day 7 iSNs in 96-well plates. **(F, G):** Side by side comparison of iSNs with AXIOGENESIS's Peri.4U sensory neurons. Images of Fluo4 loaded cells (green, F) and distribution of iSNs and Peri.4U cells in response to 1 μM capsaicin and 30 μM α,β-meATP treatment (G). **(H):** Schematic detailing the expansion of induced neural progenitor cells (iNPCs) and differentiation of iNPCs to iSNs for screening.

(NCARDIA, Gosselies, Belgium), derived from a single iPSC clone, are commercially available for assay development and toxicity screening, although they have not been thoroughly characterized in the literature. We performed a side-by-side functional comparison between the Peri.4U cells and adult PB derived iSNs. SNs were morphologically similar (Fig. 3F) and their response to capsaicin and α,β-meATP was equivalent in multiwell screening format plates (Fig. 3G), revealing that iSNs are functionally equivalent to human iPSCs at this depth of analysis.

In order to set-up a high-throughput system that is suitable for drug screening for chemotherapy-induced PN, we determined whether iSNs generation from nonmobilized PB was sufficient and at what capacity. Our optimized iNPC expansion protocol requires 2.4 M iNPCs to seed 24-well plates, which expand to confluence at 12 M iNPCs within 4–5 days—equating to a doubling time of approximately 48 hours. When expanding iNPCs, these 12 M iNPCs are split to five further 24-well plates and continue expanding. If the iNPCs are to be used for screening, the media is exchanged for snSpec media for a week, then snMat media for 2 weeks. At this stage, there are sufficient iSNs to seed six 96-well plates at 50K cells per well (Fig. 3H). A key advantage of direct conversion technologies over iPSCs such as commercially available

Axiogenesis Peri.4U precursor cells is the ability to first expand iNPC cultures, and use these expanded iNPCs to achieve cost-effective, large-scale production of differentiated iSNs.

High-Content Response of Human iSNs to Chemotherapeutic Agents

Using iSNs converted from cord blood, a dose-dependent reduction in neurite length was previously demonstrated in response to the chemotherapeutic agent Taxol as an in vitro surrogate for chemotherapy induced PN [34]. To determine whether this response was specific for Taxol and was similar to iSNs derived from adult PB, we evaluated a series of compounds (Table 2) associated with chemotherapy-induced PN from a variety of chemotherapy classes that also account for various effects on neurite degeneration of human nociceptors acting via different modes of action [6, 7]. Endpoints included cell count and neurite length measurement with automated high-content imaging, as well as independent assessments of cell viability (metabolism) using the resazurin reduction assay (Supporting Information Fig. S4A).

To distinguish between unspecific cytotoxicity and specific effects on neurite degeneration of the iSNs in a high-throughput system, an effective dosage range was determined by using a concentration-dependent inhibition of resazurin reduction (Fig. 4A). Resulting dose–response curves were used to define IC_{50} concentrations for the assessment of specific drug effects (Table 2). Forty-eight hours after treatment with the selected chemotherapeutic agents of iSNs were quantified and neurite length was measured and analyzed by high-content imaging (Fig. 4B, 4C, Supporting Information Fig. S4B) as described (Materials and Methods section). Four out of five tested compounds (Taxol, Etoposide, Vincristine, and Cisplatin) exhibited similar profiles of reduced neurite length in the absence of cytotoxicity. The IC_{50}s for neurite length reductions ranged from 5 to 10 nM, with Taxol being the most potent in this model (Table 2). In contrast, the proteasome inhibitor Bortezomib was the least effective in our system showing neurite degeneration only at the highest tested concentrations (IC_{50} = approximately 4 μM), which could be linked to its documented effect on cell cycle arrest [7] (Fig. 4B, 4C). These values are toward the lower range of IC_{50}s reported for these drugs [62, 63] (Table 2) indicating that our adult PB iSN assays have high sensitivity to tested drugs.

Since iSN treatment was initiated 24 hours after seeding to 96-well plates, it remained unclear whether treatment resulted in failure of iSNs to generate neurites or whether there was degeneration of established neurites. In order to determine this, we waited 7 days after replating the cells prior to treatment with chemotherapeutics (Supporting Information Fig. S4A). All the tested drugs affected the cells' morphology and significantly reduced the neurite length (Fig. 4D), indicating that the cells exhibited neurite degeneration, the clinical "biomarker" of chemotherapy-induced peripheral neuropathy (CIPN). These results suggest this platform would allow for high-content screening of chemotherapeutic insult to human SNs, and could be generated from adult PB in a patient specific manner of precision-based therapy toward treatment block or repair of CIPN effects to SNs.

DISCUSSION

Our study shows for the first time that direct conversion of conventional adult PB (without mobilization drug administration) to

sensory neurons is a practical way to generate sufficient quantities of sensory neurons for small molecule screening or chemogenomic campaigns for sensory neuron studies. The development of effective treatment for human pain is anchored by current clinical studies that are based on subjective human behavior-based [7] or alterative rodent models of undetermined clinical relevance [17, 64, 65]. There are numerous biological differences of nociceptive neurons between rodent and human physiology that include varied distribution in nociceptor subtypes, diverse repertoire and function of channels and receptors, altered expression of signaling molecules, and different ligand binding affinities and accessory protein interactions [19]. These distinctions between human versus nonhuman models of nociceptors may contribute invalid and/or false negative or positive targets identified through rodents studies used to derived human therapeutics. Therefore, tests investigating and modeling key mechanistic aspects of human chronic pain would benefit from a robust platform based on human specific nociceptors.

We report here on a high-throughput, in vitro screening platform based on iSNs. We show evidence that adult human nonmobilized PB can be converted to functional iSNs in approximately 30 days using a transferable and robust technology. This is faster than the overall procedure from somatic cells' reprograming to pluripotent state, that requires subsequent maturation to sensory neural differentiation of ~21–30 days reprograming and another ~14–28 days to achieve sensory neural differentiation based on the published protocols [37, 38, 63, 66–68]. This timeline for iPSC does not include the time for required for iPSC isolation, expansion, and to evaluate the genomic integrity of iPSC [69] or clone to clone variations [70, 71].

We demonstrated the ability to generate intermediate iNPCs from adult PB that can be cryopreserved and subsequently expanded for specification into iSNs. With the possibility of ex vivo expansion of CD34$^+$ cells derived from nonmobilized PB and the cumulative expansion of iNPCs, we can estimate that from 3 to 5 ml PB after 10 passages we can achieve a total of 100 M iNPCs; this represents a calculated overall yield of 10×10^9 iNPCs from all clones derived from 200 ml of adult PB. Larger blood draws would only benefit the technology and goal, and is more likely given specific patient consents for use of this applied technology can incorporate more than routine blood harvests. These cells expressed neural related protein markers, as well as signaling properties that are consistent with peripheral sensory neurons. A side-by-side comparison demonstrated that our iSNs are at least equivalent to human iPSC using commercially available human sensory neurons derived from iPSCs. Use of direct conversion technology has the advantages to overcome challenges that arise from PSCs culture and SN differentiation. These difficulties include genetic drift given prolonged cultures and freeze thaw cycle of PSCs [70, 71] and pluripotent development potential of PSCs where differentiated progeny from PSCs still contain undifferentiated cells [72] and other lineages for example, blood, muscle, and so forth, that require selective pressures, and serial passages regardless of the culture conditions (feeder-free vs. feeder layers) used. Moreover, as it has been recently published, iPSCs culture conditions prior to differentiation influence sensory neural differentiation and cause variations within the differentiated cell phenotypes [66]. This study from Schwartzentruber et al. [66] underscores the importance of considering differentiation-induced variability when using iPSCs technology for disease modeling and/or high throughput screening

Table 2. Chemotherapeutic drugs implicated in chemotherapy-induced peripheral neuropathy

Compound class	Name	Mode of action	Types of cancer treated	Neurotoxic dose in patients (mg/m²)	NP incidence (%)	Reference	Reported neurite length IC₅₀ (μM)	Detected cell viability IC₅₀ (μM)	Detected neurite length IC₅₀ (μM)
Taxanes	Paclitaxel/ Taxol/Onxol	Inhibit microtubule depolymerization, mitotic arrest	Breast, ovarian, lung, prostate, pancreatic	200–250	11–87	[7, 57–60]	0.0056–0.01	7.4	0.005
Topoisomerase inhibitors	Etoposide/ Etopophos	Interfere with the breakage-reunion reaction of DNA topoisomerase II	Testicular, lung, lymphoma, leukemia, neuroblastoma, ovarian	NA	NA	[58, 59]	0.36	3.2	0.019
Vinca alkaloids	Vincristine/ Leurocristine/ Oncorin	Inhibit microtubule polymerization, mitotic arrest	Lung, brain, bladder, testicular	5–15	Up to 20	[57, 58]	0.0055–0.002	0.6	0.063
Platinum-based	Cisplatin/ Platinol	Cancer-cell DNA-crosslinking, bind to DNA, cell cycle arrest, apoptosis	Lung, ovarian, bladder, germ cells, testicular, colorectal	250–350	70–100	[7, 57, 58]	>100	3.1	0.005
Proteasome inhibitors	Bortezomib/ Velcade	Inhibit proteasome degradation, cycle arrest, enhance microtubule polymerization	Multiple myeloma	30	20–30	[7, 57, 58, 61]	>100	1	4.2

Summarized characteristics of neurotoxicity-inducing drugs routinely used in cancer treatment. List of cancers treated is by no means exclusive, rather we point out the most frequently treated cancers assigned to a given drug or a group of drugs. The dose–response values (IC₅₀) of cell viability (Resazurin reduction), and neurite total length per neuron for induced sensory neuron cells treated with various classed of chemotherapeutic drugs for 48 hours. Each data point represents the mean ± SEM; $n = 3$ for independent experiments. Abbreviation: NA, not applicable.

studies; and in order to draw conclusions, which iPSC variants exhibit a detectable cellular phenotype, a large (40+) patient number is needed. These are not issues that impact direct conversion from blood to SNs, given the more restricted cell fate, as well as avoiding PSC culture systems that introduce variations over passage. To be able to compare 40+ patients, with our direct conversion system it would be more achievable taking that generation of iSNs is faster and cheaper with direct conversion from blood. Moreover, human iSNs exclusively expressed PRPH and Tuj1, and appeared to devoid of CNS or astroglial markers indicating a highly purified culture. We revealed that 0.5 M iSNs could be generated for a 96-well format for high-content screening of genetic or chemical targets of human SN behavior and response; the large scale expansion at the iNPC stage and a faster achievable and pure iSN culture enabled the development of a robust, repeatable and reliable in vitro high-content screening platform.

Using this platform, treatment with representative chemotherapeutic agents known to cause PN in humans reduced the neurite length of iSNs in vitro in the absence of cytotoxicity. Our assay could distinguish between effects on neurite growth vs. neurite degeneration when iSNs were treated with different agents with different mode of actions. In the case of taxanes, vinca alkaloids, and platinum-based drug classes that primary affect the axonal microtubules, we observed inhibition of neurite growth and also neurite degeneration at low concentrations consistent with previous reports. In contrast to proteasome inhibitor bortezomib, and topoisomerase inhibitor etoposide, which do not act directly on axonal structures and maintenance of axonal processes, we detected effects on neurite degeneration only at higher tested concentrations. Moreover, the effects on neurite length reduction were detected at the same or in lower concentration ranges that are used clinically.

Future direction should explore whether the observed effects on neurite outgrowth and degeneration is reversible after removal of the drugs, as it has been shown in patients that the side effects are almost reversible upon treatment discontinuation [73]. Moreover, establishing dose–response kinetics of the tested drugs and including other classes such as immunomodulatory drugs are other noteworthy approaches for future studies. Additionally, since we can generate both CNS and PNS neurons using direct conversion, it would be interesting to evaluate the drugs' possibly different effects on both neuronal cell types. Our high-throughput platform technology and protocol reported here could serve as a suitable tool for more complex studies of phenotypic readouts for target/pathway validation and large single or combinatorial compound screens. Overall, our high-throughput in vitro system can provide a viable screen for candidate compound that will prevent, block, or repair chemotherapeutic agent damage in a model of CIPN and secondary level of assays that will identify which mechanisms and mode of actions are involved.

CONCLUSION

Our study provides a system and methodology to derive and interrogate human SNs from human adult PB for the scientific community. Using direct conversion from CD34+ stem/progenitors of the hematopoietic system, we illustrate the potential to generate 100-million neural progenitor cells that can be used to derive iSNs in 96-well format for subsequent screening. We propose the platform can be applied to high throughput phenotypic screening campaigns for drug discovery and
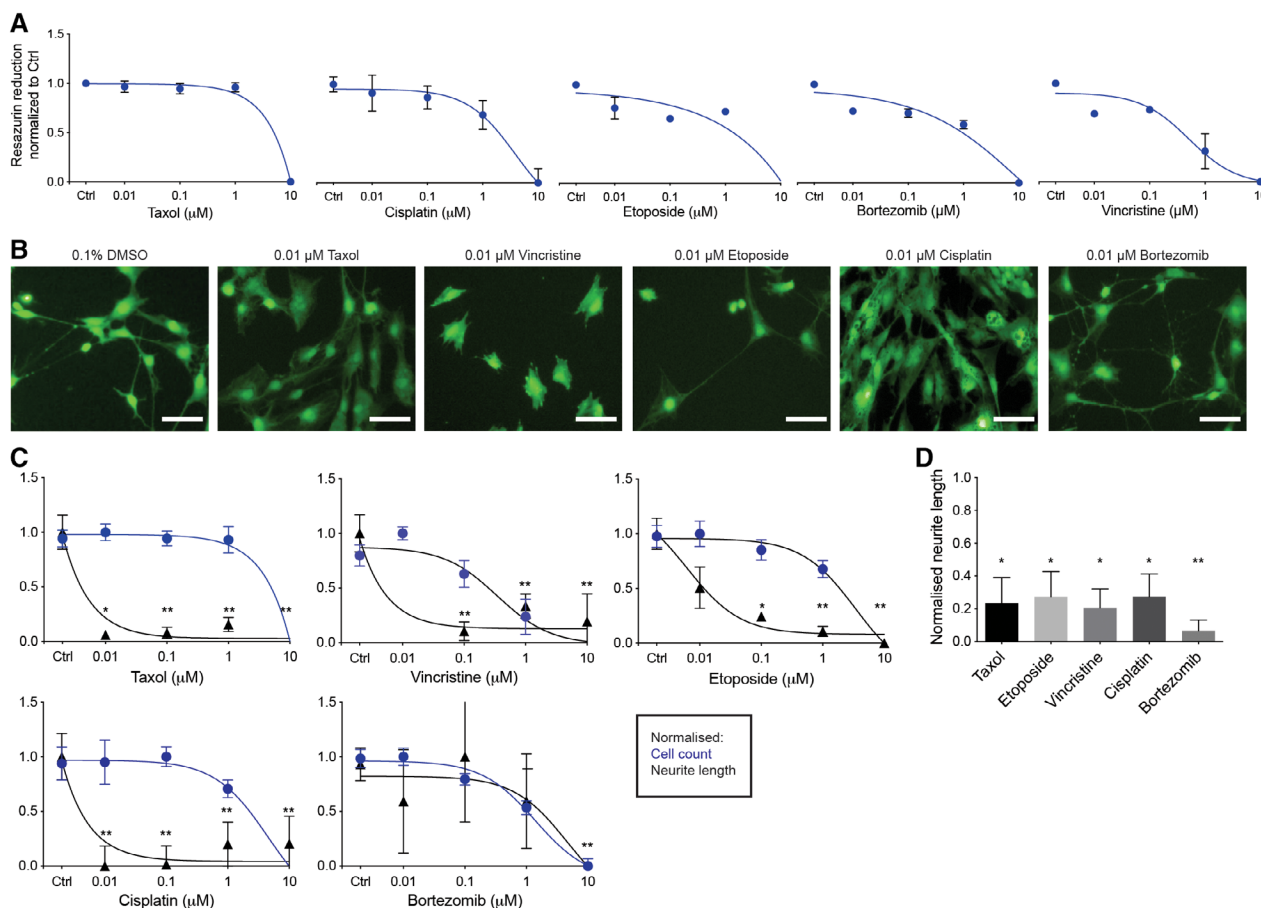
Figure 4. Assessment of various chemotherapy compounds in the induced sensory neurons (iSNs). **(A):** Resazurin based cytotoxicity. Differentiated iSNs were exposed to four doses of different chemotherapeutic agents (0.01–10 μM) for 48 hours. Data are given as mean ± SEM of three replicates. **(B):** Representative images of calcein green stained iSNs treated with different chemotherapeutic agents at 0.01 μM concentration for 48 hours. Cells were treated 24 hours after seeding. Scale bar represents 50 μM. **(C):** Normalized dose-dependent neurite length and cell count. Each data point represents the mean ± SEM, $n = 3$ independent experimental runs (biological replicates). Statistical significance was considered at $p < .05$, where *, $p = .05$ and **, $p = .01$. **(D):** Neurite degeneration. Normalized neurite length of iSNs 7 days after seed treated with different chemotherapeutic agents at IC_{50} concentrations. Data are given as mean ± S.E.M of three replicates. Statistical significance was considered at $p < .05$, where *, $p = .05$ and **, $p = .01$.

chemogenomic approaches to elucidate unknown mode of actions of neurodevelopmental disorders, such as neuropathy, as well the study of the phenotype, gene expression, or functionality of iNPC-derived nociceptive neurons in genetic screens to identify new human specific targets of nociceptive control.

AUTHOR CONTRIBUTIONS

K.V.: conception and design, experimental work, collection and/or assembly of data, data analysis and interpretation, manuscript writing; S.M.: experimental work, collection and/or assembly of related data, data analysis; T.J.C.: experimental design, project supervision, data analysis and interpretation, manuscript writing; M.B.: conception and design, project supervision, manuscript writing, final editing and oversight manuscript.

DISCLOSURE OF POTENTIAL CONFLICTS OF INTEREST

The authors indicated no potential conflicts of interest.

DATA AVAILABILITY STATEMENT

The data that support the findings of this study are available from the corresponding author upon reasonable request.

References

1 Hughes RA. Peripheral neuropathy. BMJ 2002;324:466–469.

2 Merskey H. Clarifying definition of neuropathic pain. Pain 2002;96:408–409.

3 Kernich CA. Patient and family fact sheet. Peripheral neuropathy. Neurologist 2001;7:315–316.

4 National Institute of Neurological Disorders and Stroke. Peripheral Neuropathy Fact Sheet. 2018.

5 Lema MJ, Foley KM, Hausheer FH. Types and epidemiology of cancer-related neuropathic pain: The intersection of cancer pain and neuropathic pain. Oncologist 2010;15:3–8.

6 Addington J, Freimer M. Chemotherapy-induced peripheral neuropathy: An update on the current understanding. F1000Res 2016;5:F1000 Faculty Rev-1466.

7 Fukuda Y, Li Y, Segal RA. A mechanistic understanding of axon degeneration in chemotherapy-induced peripheral neuropathy. Front Neurosci 2017;11:481.

8 Boyette-Davis JA, Cata JP, Zhang H et al. Follow-up psychophysical studies in bortezomib-related chemoneuropathy patients. J Pain 2011;12:1017–1024.

9 Wolf S, Barton D, Kottschade L et al. Chemotherapy-induced peripheral neuropathy: Prevention and treatment strategies. Eur J Cancer 2008;44:1507–1515.

10 Argyriou AA, Assimakopoulos K, Iconomou G et al. Either called "chemobrain" or "chemofog," the long-term chemotherapy-induced cognitive decline in cancer survivors is real. J Pain Symptom Manage 2011;41:126–139.

11 Binda D, Vanhoutte EK, Cavaletti G et al. Rasch-built Overall Disability Scale for patients with chemotherapy-induced peripheral neuropathy (CIPN-R-ODS). Eur J Cancer 2013;49:2910–2918.

12 Moulin D, Boulanger A, Clark AJ et al. Pharmacological management of chronic neuropathic pain: Revised consensus statement from the Canadian Pain Society. Pain Res Manag 2014;19:328–335.

13 Majithia N, Temkin SM, Ruddy KJ et al. National Cancer Institute-supported chemotherapy-induced peripheral neuropathy trials: Outcomes and lessons. Support Care Cancer 2016;24:1439–1447.

14 Finnerup NB, Attal N, Haroutounian S et al. Pharmacotherapy for neuropathic pain in adults: A systematic review and meta-analysis. Lancet Neurol 2015;14:162–173.

15 Kumar A, Kaur H, Singh A. Neuropathic pain models caused by damage to central or peripheral nervous system. Pharmacol Rep 2018;70:206–216.

16 Sapunar D, Puljak L. What can rats tell us about neuropathic pain? Critical evaluation of behavioral tests used in rodent pain models. Period Biol 2009;111:155–160.

17 Hoke A, Ray M. Rodent models of chemotherapy-induced peripheral neuropathy. ILAR J 2014;54:273–281.

18 Large D. Unraveling chemotherapy-induced peripheral neuropathy: in vitro and in vivo models of sensory nerve dysfunction. J Neurosci Res 2018;96:1739–1740.

19 Davidson S, Copits BA, Zhang J et al. Human sensory neurons: Membrane properties and sensitization by inflammatory mediators. Pain 2014;155:1861–1870.

20 Takahashi K, Tanabe K, Ohnuki M et al. Induction of pluripotent stem cells from adult human fibroblasts by defined factors. Cell 2007;131:861–872.

21 Efe JA, Hilcove S, Kim J et al. Conversion of mouse fibroblasts into cardiomyocytes using a direct reprogramming strategy. Nat Cell Biol 2011;13:215–222.

22 Pang ZP, Yang N, Vierbuchen T et al. Induction of human neuronal cells by defined transcription factors. Nature 2011;476:220–223.

23 Szabo E, Rampalli S, Risueno RM et al. Direct conversion of human fibroblasts to multilineage blood progenitors. Nature 2010;468:521–526.

24 Theunissen TW, Powell BE, Wang H et al. Systematic identification of culture conditions for induction and maintenance of naive human pluripotency. Cell Stem Cell 2014;15:524–526.

25 Shen Y, Yue F, McCleary DF et al. A map of the cis-regulatory sequences in the mouse genome. Nature 2012;488:116–120.

26 Nichols J, Smith A. Naive and primed pluripotent states. Cell Stem Cell 2009;4:487–492.

27 Vierbuchen T, Ostermeier A, Pang ZP et al. Direct conversion of fibroblasts to functional neurons by defined factors. Nature 2010;463:1035–1041.

28 Yoo AS, Sun AX, Li L et al. MicroRNA-mediated conversion of human fibroblasts to neurons. Nature 2011;476:228–231.

29 Pfisterer U, Kirkeby A, Torper O et al. Direct conversion of human fibroblasts to dopaminergic neurons. Proc Natl Acad Sci USA 2011;108:10343–10348.

30 Son EY, Ichida JK, Wainger BJ et al. Conversion of mouse and human fibroblasts into functional spinal motor neurons. Cell Stem Cell 2011;9:205–218.

31 Caiazzo M, Dell'Anno MT, Dvoretskova E et al. Direct generation of functional dopaminergic neurons from mouse and human fibroblasts. Nature 2011;476:224–227.

32 Wainger BJ, Buttermore ED, Oliveira JT et al. Modeling pain in vitro using nociceptor neurons reprogrammed from fibroblasts. Nat Neurosci 2015;18:17–24.

33 Wang H, Zhao S, Finnell RH et al. Generation of integration-free induced pluripotent stem cells from a patient with spina bifida. Stem Cell Res 2018;31:27–30.

34 Lee JH, Mitchell RR, McNicol JD et al. Single transcription factor conversion of human blood fate to NPCs with CNS and PNS developmental capacity. Cell Rep 2015;11:1367–1376.

35 Tanabe K, Ang CE, Chanda S et al. Transdifferentiation of human adult peripheral blood T cells into neurons. Proc Natl Acad Sci USA 2018;115:6470–6475.

36 Yu KR, Shin JH, Kim JJ et al. Rapid and efficient direct conversion of human adult somatic cells into neural stem cells by HMGA2/let-7b. Cell Rep 2015;10:441–452.

37 Chambers SM, Qi Y, Mica Y et al. Combined small-molecule inhibition accelerates developmental timing and converts human pluripotent stem cells into nociceptors. Nat Biotechnol 2012;30:715–720.

38 Guo X, Spradling S, Stancescu M et al. Derivation of sensory neurons and neural crest stem cells from human neural progenitor hNP1. Biomaterials 2013;34:4418–4427.

39 Lee KS, Zhou W, Scott-McKean JJ et al. Human sensory neurons derived from induced pluripotent stem cells support varicella-zoster virus infection. PloS One 2012;7:e53010.

40 Giorgetti A, Marchetto MC, Li M et al. Cord blood-derived neuronal cells by ectopic expression of Sox2 and c-Myc. Proc Natl Acad Sci USA 2012;109:12556–12561.

41 Castano J, Menendez P, Bruzos-Cidon C et al. Fast and efficient neural conversion of human hematopoietic cells. Stem Cell Rep 2014;3:1118–1131.

42 Tang X, Wang S, Bai Y et al. Conversion of adult human peripheral blood mononuclear cells into induced neural stem cell by using episomal vectors. Stem Cell Res 2016;16:236–242.

43 Mitchell RR, Szabo E, Benoit YD et al. Activation of neural cell fate programs toward direct conversion of adult human fibroblasts into tri-potent neural progenitors using OCT-4. Stem Cells Dev 2014;23:1937–1946.

44 Guimaraes MZP, De Vecchi R, Vitoria G et al. Generation of iPSC-derived human peripheral sensory neurons releasing substance P elicited by TRPV1 agonists. Front Mol Neurosci 2018;11:277.

45 Ying QL, Stavridis M, Griffiths D et al. Conversion of embryonic stem cells into neuroectodermal precursors in adherent monoculture. Nat Biotechnol 2003;21:183–186.

46 Denham M, Hasegawa K, Menheniott T et al. Multipotent caudal neural progenitors derived from human pluripotent stem cells that give rise to lineages of the central and peripheral nervous system. Stem Cells 2015;33:1759–1770.

47 Denham M, Dottori M. Neural differentiation of induced pluripotent stem cells. Methods Mol Biol 2011;793:99–110.

48 Alshawaf AJ, Viventi S, Qiu W et al. Phenotypic and functional characterization of peripheral sensory neurons derived from human embryonic stem cells. Sci Rep 2018;8:603.

49 Cho T, Chaban VV. Interaction between P2X3 and oestrogen receptor (ER)alpha/ERbeta in ATP-mediated calcium signalling in mice sensory neurones. J Neuroendocrinol 2012;24:789–797.

50 Xu GY, Huang LY. Peripheral inflammation sensitizes P2X receptor-mediated responses in rat dorsal root ganglion neurons. J Neurosci 2002;22:93–102.

51 Wu D, Yang P, Zhang X et al. Targeting a dominant negative rho kinase to neurons promotes axonal outgrowth and partial functional recovery after rat rubrospinal tract lesion. Mol Ther 2009;17:2020–2030.

52 Chan CC, Khodarahmi K, Liu J et al. Dose-dependent beneficial and detrimental effects of ROCK inhibitor Y27632 on axonal sprouting and functional recovery after rat spinal cord injury. Exp Neurol 2005;196:352–364.

53 Watzlawick R, Sena ES, Dirnagl U et al. Effect and reporting bias of RhoA/ROCK-blockade intervention on locomotor recovery after spinal cord injury: A systematic review and meta-analysis. JAMA Neurol 2014;71:91–99.

54 Jia XF, Ye F, Wang YB et al. ROCK inhibition enhances neurite outgrowth in neural stem cells by upregulating YAP expression in vitro. Neural Regen Res 2016;11:983–987.

55 Boomkamp SD, Riehle MO, Wood J et al. The development of a rat in vitro model of spinal cord injury demonstrating the

additive effects of Rho and ROCK inhibitors on neurite outgrowth and myelination. Glia 2012;60:441–456.

56 Koyanagi M, Takahashi J, Arakawa Y et al. Inhibition of the Rho/ROCK pathway reduces apoptosis during transplantation of embryonic stem cell-derived neural precursors. J Neurosci Res 2008;86:270–280.

57 Banach M, Juranek JK, Zygulska AL. Chemotherapy-induced neuropathies-a growing problem for patients and health care providers. Brain Behav 2017;7:e00558.

58 Grisold W, Cavaletti G, Windebank AJ. Peripheral neuropathies from chemotherapeutics and targeted agents: Diagnosis, treatment, and prevention. Neuro Oncol 2012;14:iv45–iv54.

59 Scripture CD, Figg WD, Sparreboom A. Peripheral neuropathy induced by paclitaxel: Recent insights and future perspectives. Curr Neuropharmacol 2006;4:165–172.

60 Song SJ, Min J, Suh SY et al. Incidence of taxane-induced peripheral neuropathy receiving treatment and prescription patterns in patients with breast cancer. Support Care Cancer 2017;25:2241–2248.

61 Meregalli C. An overview of bortezomib-induced neurotoxicity. Toxics 2015;3: 294–303.

62 Han C, Qi J, Shi X et al. Prostaglandins from a zoanthid: Paclitaxel-like neurite-degenerating and microtubule-stabilizing activities. Biosci Biotechnol Biochem 2006;70: 706–711.

63 Rana P, Luerman G, Hess D et al. Utilization of iPSC-derived human neurons for high-throughput drug-induced peripheral neuropathy screening. Toxicol In Vitro 2017;45:111–118.

64 Mogil JS. Animal models of pain: Progress and challenges. Nat Rev Neurosci 2009; 10:283–294.

65 Vierck CJ, Hansson PT, Yezierski RP. Clinical and pre-clinical pain assessment: Are we measuring the same thing? Pain 2008;135:7–10.

66 Schwartzentruber J, Foskolou S, Kilpinen H et al. Molecular and functional variation in iPSC-derived sensory neurons. Nat Genet 2018;50:54–61.

67 Malik N, Rao MS. A review of the methods for human iPSC derivation. Methods Mol Biol 2013;997:23–33.

68 Kogut I, McCarthy SM, Pavlova M et al. High-efficiency RNA-based reprogramming of human primary fibroblasts. Nat Commun 2018;9:745.

69 D'Antonio M, Benaglio P, Jakubosky D et al. Insights into the mutational burden of human induced pluripotent stem cells from an integrative multi-omics approach. Cell Rep 2018;24:883–894.

70 Liang G, Zhang Y. Genetic and epigenetic variations in iPSCs: Potential causes and implications for application. Cell Stem Cell 2013;13:149–159.

71 Kilpinen H, Goncalves A, Leha A et al. Common genetic variation drives molecular heterogeneity in human iPSCs. Nature 2017; 546:370–375.

72 Ben-David U, Benvenisty N. The tumorigenicity of human embryonic and induced pluripotent stem cells. Nat Rev Cancer 2011; 11:268–277.

73 Staff NP, Grisold A, Grisold W et al. Chemotherapy-induced peripheral neuropathy: A current review. Ann Neurol 2017;81: 772–781.

See www.StemCellsTM.com for supporting information available online.